INT. J. NUM. METH. HEAT FLUID FLOW, VOL. 2, 359–370 (1992)

FLOW OF THE POWER-LAW FLUID IN THE INLET REGION OF A DUCT WITH BLOWING OR SUCTION

C. I. HUNG AND Y. Y. PERNG

Department of Mechanical Engineering, National Cheng-Kung University, Tainan, Taiwan, Republic of China

ABSTRACT

The hydrodynamic development of non-Newtonian fluid flow in the entrance region of a duct with porous walls is examined numerically by solving the modified Navier–Stokes equations. Cases involving blowing, suction, and no mass transfer through the walls are considered. Velocity distributions, pressure drops, and skin friction coefficients are presents for each case. A definite concavity is found in the velocity profile near the duct entrance for all cases. Results for Newtonian fluids are compared with previous studies in which boundary-layer theory was used. In the region away from the entrance it is found that the present results are in good agreement with previous works. In the region close to the entrance, or in the case of suction, boundary-layer theory is shown to be inappropriate.

KEY WORDS Duct inlet Navier–Stokes equations Non-Newtonian fluid flow

NOMENCLATURE

b	half-duct width
C_f	wall skin friction coefficient, $\left.\frac{\tau_{xy}}{\frac{1}{2}\rho u_0^2}\right\|_{y=b}$
K	consistency index
L	duct length
n	flow index of power-law fluid
p	pressure
P	dimensionless pressure, $p/\rho u_0^2$
Re	Reynolds number, $[\rho u_0^{2-n}.(2b)^n]/K$
u	dimensional axial velocity
U	dimensionless axial velocity, u/u_o
v	dimensional transverse velocity
V	dimensionless transverse velocity, v/u_0
x	dimensional axial coordinate
Y	dimensionless transverse coordinate, y/b
y	dimensional transverse coordinate
Y	dimensionless transverse coordinate, y/b

Greek

τ_{xy}	shear stress on a fluid element
μ_a	apparent viscosity
η	dimensionless apparent viscosity

Superscript

–	average

Subscripts

c	centreline condition
o	inlet condition
w	wall conditions

INTRODUCTION

Due to the importance of non-Newtonian fluid in the processing of molten plastics, polymers, etc., considerable research efforts have been conducted to understand the behaviour of these fluids. In the flow of a fluid through a channel, the velocity distribution undergoes a development from some initial profile at the inlet to a fully-developed profile at locations far downstream.

0961–5539/92/040359–12$2.00

Received April 1991
Revised December 1991

Correspondingly, the pressure gradient in the region of flow development will differ from that of a fully developed flow. Therefore, it is of considerable interest to determine the detailed nature of velocity development in the entrance region.

Numerous papers are found in the literature which deal with analytical, numerical, and experimental studies of entrance flow for non-Newtonian fluids. The analytical solutions for the velocity profiles, obtained by the linearization of the momentum equations, is given by Langhaar[1] for the circular tube. Sparrow *et al.*[2] extended this approach to calculate the laminar flow development and pressure drops in the entrance region of tubes and ducts. Collins and Schowalter[3] employed a perturbation technique to study the flow development of non-Newtonian fluids in a channel. The Karman–Pohlhausen momentum integral method was first applied to the entrance-region problem by Schiller[4]. Gupta[5] applied a similar approach to the case of pseudoplastic fluids. A variational technique was used by Tomita[6] to investigate the entrance-region flow of power-law fluids at low Reynolds numbers.

A further approach is to obtain numerical solutions by finite difference techniques. Duda and Vrentas[7] used this method to study the entrance-region flow of a Powell–Eyring non-Newtonian fluid. The inlet region for laminar flow in porous pipes with small rates of injection or suction has been analysed numerically by Hornbeck *et al.*[8].

While boundary layer theory has been extensively used for entrance flow problems, its assumptions are invalid near the entrance of the tube. Solutions of the full Navier–Stokes equations near the entrance of a tube differ from the boundary layer solutions. The numerical solutions of the Navier–Stokes equations in the entrance region have been obtained by Wang and Longwell[9], McDonald *et al.*[10], and Koyari *et al.*[11]; but these authors did not consider blowing or suction and they did not consider non-Newtonian fluids.

In this paper we investigate the hydrodynamic development of a power-law non-Newtonian fluid in a duct with wall injection and suction. Since the boundary-layer assumptions are not valid near the entrance region, the modified Navier–Stokes equations are solved numerically. The modified equations used for power-law liquid are different from the conventional Navier–Stokes equations by that the viscosity of a power-law liquid is dependent on the shear rate but the Newtonian viscosity is independent of the shear rate[12]. The relation of shear stress to rate-of-shear-strain of the power-law non-Newtonian fluids is:

$$\mu_a = K\left\{2\left[\left(\frac{\partial u}{\partial x}\right)^2 + \left(\frac{\partial v}{\partial y}\right)^2\right] + \left(\frac{\partial u}{\partial y} + \frac{\partial v}{\partial x}\right)^2\right\}^{(n-1)/2} \tag{1}$$

where μ_a is the apparent viscosity, K the consistency index, and n the flow index. For $n=1$, the above equation reduces to the Newtonian case, i.e. $\mu_a = K =$ constant. For n other than 1 and at a given ratio of shear stress to rate-of-shear-strain, the larger flow index n, the greater grows the apparent viscosity. Results are presented for a Reynolds number of 100. These results are not currently available in the existing literature.

ANALYSIS

Mathematical formulation

Consider steady, laminar isothermal flow of an incompressible non-Newtonian fluid in the entrance region of a plane duct with porous walls. The flow is two-dimensional and is uniform at the entrance. The fluid which is injected in is assumed to be identical to the fluid flowing in the duct.

The geometry being considered is shown in *Figure 1*. The duct width is $2b$ and a cartesian coordinate system with its origin at the inlet is used. The x axis is on the duct centreline, and the y axis is normal to the centreline.

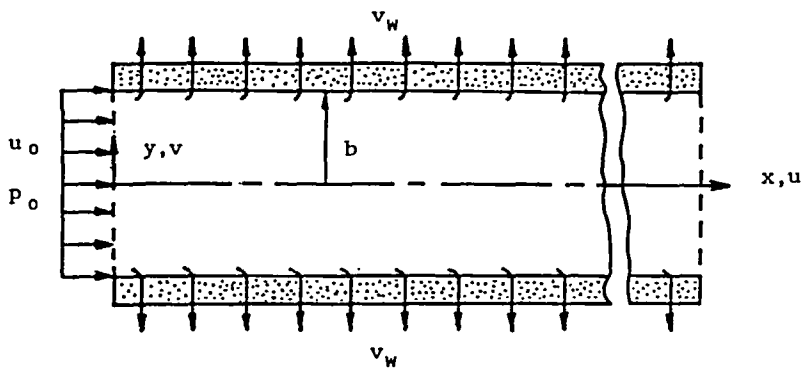

Figure 1 Schematic of the physical situation

The dimensionless varibles chosen are:

$$X=x/b, \qquad Y=y/b, \qquad U=u/u_o \tag{2a}$$

$$V=v/u_o, \qquad P=p/\rho u_o^2 \tag{2b}$$

The corresponding non-dimensional governing equations are expressed as follows:
continuity equation:

$$\frac{\partial U}{\partial X}+\frac{\partial V}{\partial Y}=0 \tag{3}$$

X-*momentum equation*:

$$\partial(UU)/\partial X+\partial(UV)/\partial Y=-\partial P/\partial X+2^n/Re.[\partial(\eta.\partial U/\partial X)/\partial X+\partial(\eta.\partial U/\partial Y)/\partial Y]+ 2^n/Re.[\partial(\eta.\partial U/\partial X)/\partial X+\partial(\eta.\partial V/\partial X)/\partial Y] \tag{4}$$

Y-*momentum equation*:

$$\partial(UV)/\partial X+\partial(VV)/\partial Y=-\partial P/\partial Y+2^n/Re.[\partial(\eta.\partial V/\partial X)/\partial X+\partial(\eta.\partial V/\partial Y)/\partial Y]+ 2^n/Re.[\partial(\eta.\partial U/\partial Y)/\partial X+\partial(\eta.\partial V/\partial Y)/\partial Y] \tag{5}$$

where

$$Re=\frac{\rho u_o^{2-n}(2b)^n}{K} \tag{6a}$$

$$\eta=\{2[(\partial U/\partial X)^2+(\partial V/\partial Y)^2]+(\partial U/\partial Y+\partial V/\partial X)^2\}^{(n-1)/2} \tag{6b}$$

Note that for $n=1$, the above system reduces to the conventional Navier–Stokes equations for a Newtonian fluid.

Because of symmetry, only the region between the wall ($Y=1$) and the centreline ($Y=0$) need to be considered. Non-dimensional boundary conditions employed in the present study are described as follows.

Inlet: $U=1, \quad V=0$ (7a)

Walls: $U=0, \quad V=V_w$ (7b)

Symmetry axis: $\partial U/\partial Y=0, \quad V=0$ (7c)

Condition (6a) specifies that the inlet flow is uniform and parallel. In (6b), the no-slip condition at the wall and the blowing or suction velocity at the wall are given. For blowing, V_w is defined to be negative; for suction, V_w is positive.

The boundary condition at the exit is different for blowing and suction[13]:

For $V_w > 0$: $U = 0, \quad \partial V/\partial X = 0$ (7d)

For $V_w \leqslant 0$: $V = 0, \quad \partial(U/\bar{U})/\partial X = 0$ (7e)

where $\bar{U}$ represents the average dimensionless axial velocity. For $V_w > 0$, the fluid inside the duct is taken out continuously through wall suction, and becomes empty at $x/b = L = Re/V_w$. The flow for $x/b > L$ can be envisioned as a mirror image of that for $x/b < L$, making $x/b = L$ a plane of symmetry. Physically this situation would occur when the duct was open at both ends so that the fluid moves axially inward symmetrically about the midplane ($x/b = L$) of the duct. Thus, the boundary condition at $x = L$ is adopted as (7d). For the wall blowing case, fluid is injected continuously into the duct. When the flow is fully developed, the axial velocities at exit are linearly proportional to the axial distance; this situation is stated in (7e).

Method of solution

Because of the elliptic nature of the flow, (3)–(5) are solved using an implicit finite difference procedure called SIMPLER (Semi-Implicit Method for Pressure Linked Equations, Revised). This method was developed by Patankar[14]. In this method, the domain is subdivided into a number of control volumes, each associated with a grid point, and the governing differential equations are integrated over each control volume resulting in a system of algebraic equations that can be solved by an iterative technique. All the momentum fluxes across the control surfaces are evaluated approximately by the power-law scheme. To avoid checkerboard fields, the velocities are stored at staggered locations (*Figure 2*). The pressure–velocity linkage is resolved by a predictor–corrector technique.

In the present method, the Reynolds number is not necessarily restricted to a small value. However, the larger the Reynolds number, the longer is the duct length in order to attain fully developed flow. For the sake of saving computational costs, a Reynolds number of 100 is used in the present study. Also, the entrance length for a power-law fluid is dependent on the flow index n, i.e., the entrance length is longer for a smaller value of n. In the present paper, the calculations are performed for $n = 0.6$, 0.8, 1.0, 1.2, and 1.4. For $n = 0.6$, the entrance length is[3] $x/b = 0.12Re$; but for blowing, the computational length should be longer. To ensure that the solutions are not influenced by the outlet boundary conditions, the computational duct length

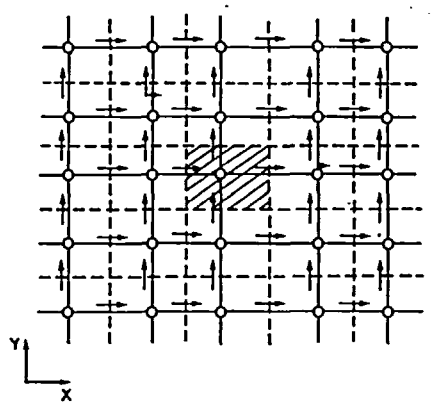

Figure 2 Staggered grid system. → for u; ↑ for v;

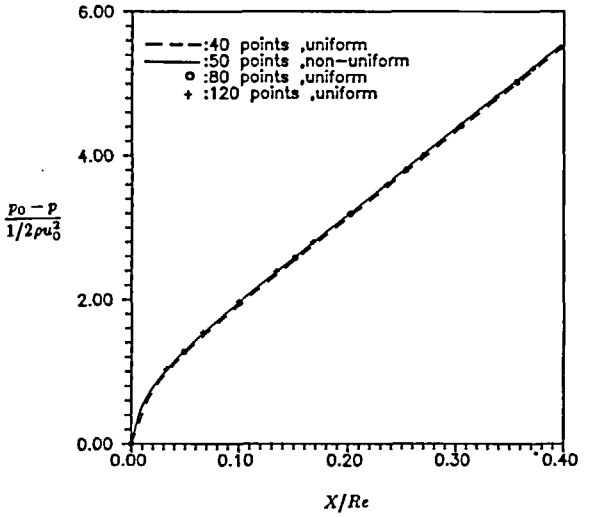

Figure 3 Test of grid-point distribution in axial direction

for $V_w<0$ (blowing) is taken as $40b$. For suction ($V_w=0.04$), the fluid becomes empty at[13] $x/b=25$; therefore, L is set equal to $25b$ in the case of suction.

To determine the appropriated grid size in the x-direction, calculations are performed on increasingly finer grid sizes. The final distribution chosen is a 50×20 non-uniform grid with a denser clustering near the wall and centreline, and near the inlet and exit of the duct. The results of grid-independency test are presented in *Figure 3* in terms of the axial-pressure distribution.

RESULTS AND DISCUSSION

Velocity distribution

In previous studies of entrance region problem, boundary-layer theory was used extensively. It is known that this approximation is not valid in the vicinity of the entrance of the duct. *Figure 4* shows the distributions of the axial velocity at the centreline for a Newtonian fluid, with $V_w=0$. Obviously, the axial diffusion term in the momentum equations cannot be neglected in the entrance region. The numerical values obtained from the modified Navier–Stokes solutions in the present work and in that by Raithby[13] are lesser than approximation by boundary layer theory, as shown in *Figure 4*. However, the trend shows good agreement.

The velocity gradient near the wall is very large. Therefore, the apparent viscosity of power-law non-Newtonian fluid becomes larger as n is increased. To satisfy the continuity equation, the axial velocity at the centre of duct should become larger as n increases. *Figure 4* also shows this trend. For fully developed flow, the theoretical values of the centreline velocity are given as[15]:

$$u_c/u_o=(2n+1)/(n+1) \tag{8}$$

The above fully developed flow value can be reached only at infinity. The comparison is given in *Table 1*. It is shown that the present results are within 1% of the fully developed flow values.

Figure 5 shows the axial velocity distributions at four different locations for $V_w=0$. It is seen that there is a noticeable effect upstream of the entrance and the velocity distribution is concave in the central portion. These velocity 'overshoots' have been determined not to be a numerical effect, but rather a valid solution[9,13]. The extent of velocity overshoots ranges from 4% to 6% higher than the centre velocities for $V_w=0$, 4.7% to 5.9% higher for $V_w=-0.04$, and 3% to

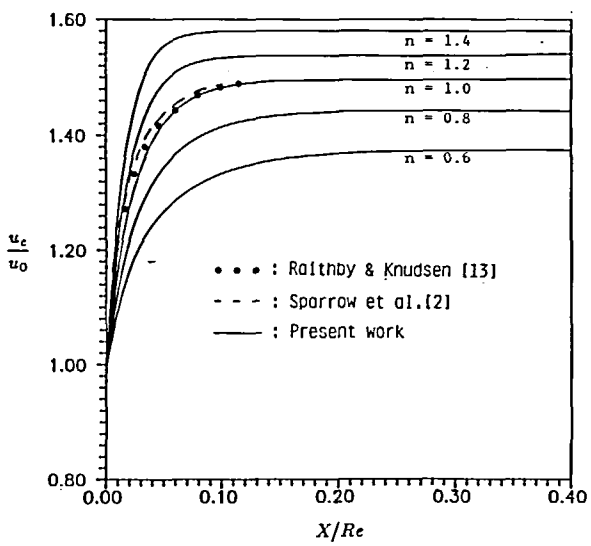

Figure 4 Centreline velocity distribution; $V_w=0$

Table 1 Comparison of fully-developed centreline velocity

n	$\frac{2n+1}{n+1}$	Present work
0.6	1.375	1.374399
0.8	1.4444	1.442666
1	1.5	1.496037
1.2	1.5454	1.540641
1.4	1.583	1.580032

Table 2 Locations of maximum centreline velocity for $V_w=0.04$

n	X/Re	$\frac{u_c}{u_o}$
0.6	0.0014507	1.036382
0.8	0.022478	1.087581
1	0.026656	1.149935
1.2	0.030969	1.222024
1.4	0.030969	1.295822

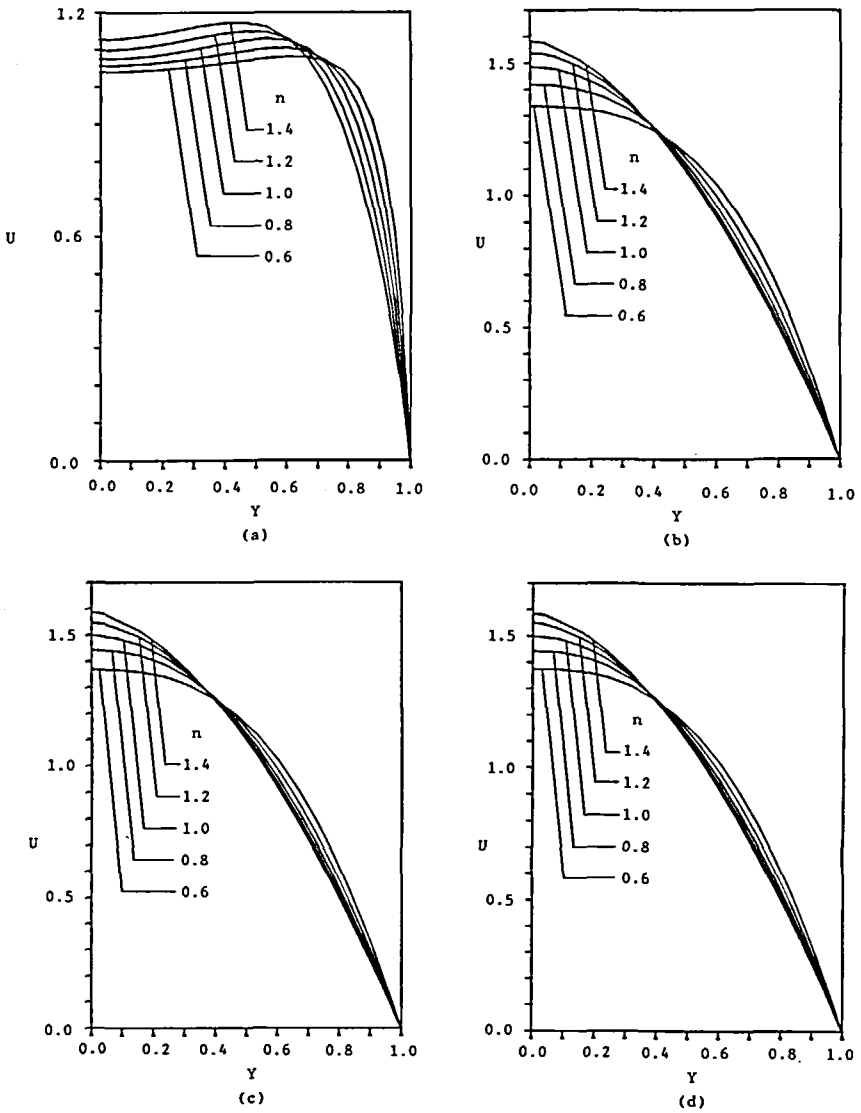

Figure 5 Velocity distributions for $V_w=0$ at (a) $X/Re=0.004364$; (b) $X/Re=0.104824$; (c) $X/Re=0.201816$; (d) $X/Re=0.4$

7% higher for $V_w=0.04$. Consequently, according to the continuity, the concavity of velocity profile indicates that the centre velocity must be lesser than that of a conventional parabolic-like profile. This explains the difference which is shown in *Figure 4*. As the length is increased, the viscous effect near the wall is diffused towards the duct centre and the concavity of velocity profile disappears gradually. The profiles which are shown in *Figures 5c* and *5d* are nearly the same. It shows that the computational length taken in the calculations is sufficient to include fully developed flow.

The centreline velocity development with wall blowing ($V_w=-0.04$) is shown in *Figure 6*. It is found that the centreline velocity increases linearly for $(x/b)>0.12Re$. This is caused by fully developed flow in this region. *Figure 7* presents axial velocity distributions at different axial locations. As before, the concavity of velocity may be noticed by referring to *Figures 5a* and *7a*.

For the case of wall suction ($V_w=0.04$), the relatively small amount of fluid being removed and the effect of wall shear give rise to an increasing centreline velocity in the vicinity of the duct entrance. Thus, the centreline velocity increases to a maximum value, then decreases to zero when the duct is empty. *Table 2* lists the axial locations of the maximum centreline velocity and *Figure 8* shows the centreline velocity distribution for various flow index n. It is seen that the maximum value of centreline velocity u_c is increased as n increases, but there is no general rule for the location of maximum u_c.

Figure 9 shows the velocity distributions at various locations for the case of wall suction. In *Figure 9a*, the concavity of velocity profile still can be found near the leading edge, but the shape is developing until the maximum value is reached (*Figure 9b*). After that the velocity decreases gradually, because the fluid is removed through the wall, as shown in *Figures 9c* and *9d*.

Compared with the case of impermeable wall ($V_w=0$), it can be seen that when the fluid is injected into the duct, the volume of fluid is increased and the fluid near the wall speeds up in the leading edge region. Hence, the position of maximum velocity is pushed away from wall. On the contrary, when fluid is removed from the duct, the fluid slows down and the location of maximum velocity is pulled towards the wall.

Skin friction coefficient

One of the important tasks in solving entrance region problem is the determination of skin

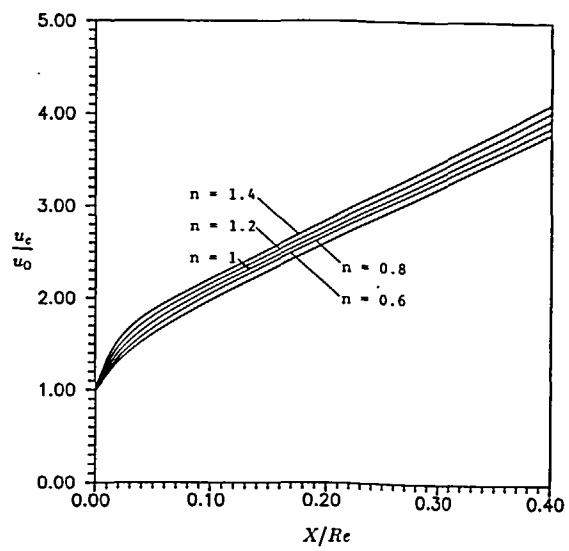

Figure 6 Centreline velocity distribution; $V_w=-0.04$

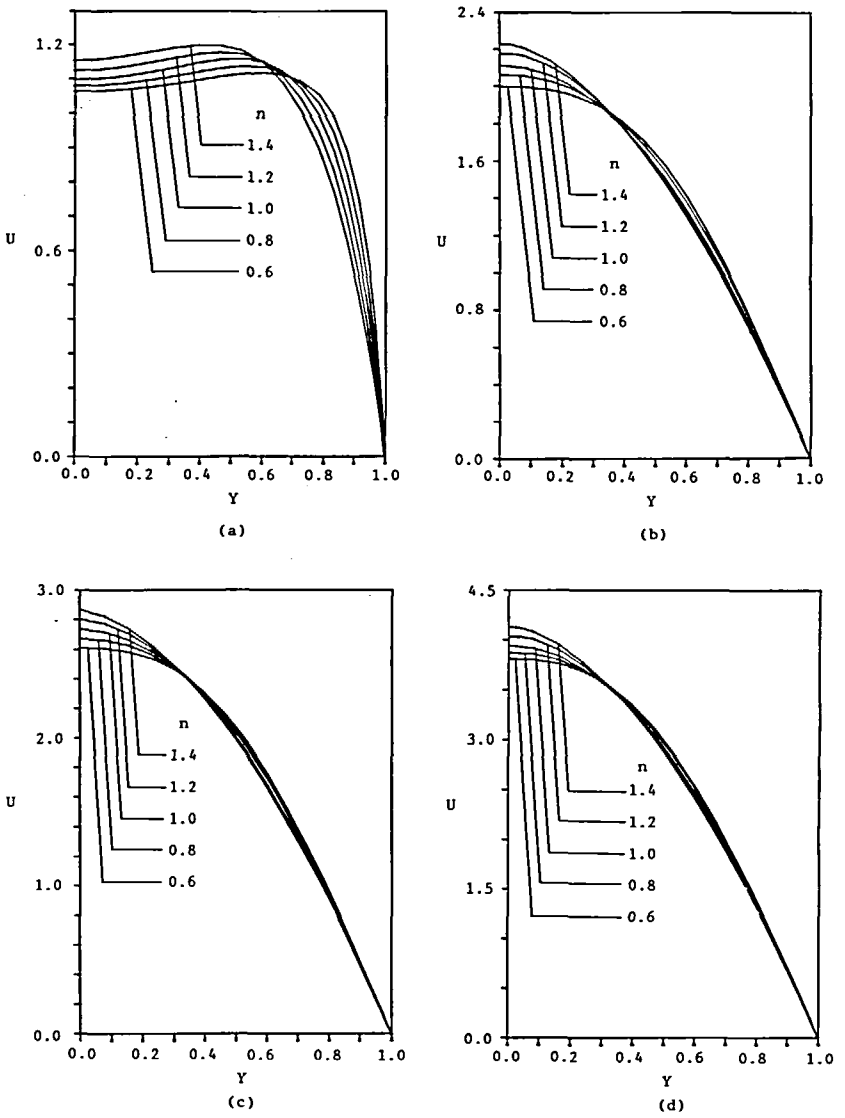

Figure 7 Velocity distributions for $V_w = -0.04$ at (a) $X/Re = 0.004364$; (b) $X/Re = 0.104824$; (c) $X/Re = 0.201816$; (d) $X/Re = 0.4$

friction coefficient which is defined as:

$$C_f = \frac{\tau_{xy}}{\frac{1}{2}\rho u_0^2}\bigg|_{y=b} \tag{9}$$

Figures 10–12 indicate the distributions of skin friction coefficient along the flow direction. In *Figure 10*, the present solution is compared with a previous study which is based on an integral solution of the boundary layer equations[16]. Good agreement is shown. Since the skin friction is a local effect near the wall, the momentum integral technique with a higher order approximation of the velocity profiles can yield accurate results as shown in *Figure 10*.

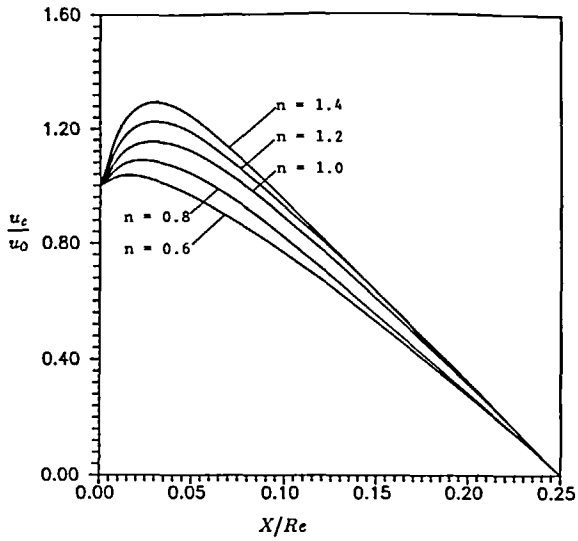

Figure 8 Centreline velocity distribution; $V_w = 0.04$

For an impermeable wall (*Figure 10*), the skin friction coefficient decreases rapidly to a minimum, and then approaches a constant value. In the case of wall blowing (*Figure 11*), the volume of fluid inside the duct is increasing; therefore, the skin friction coefficient decreases first to minimum, then increases downstream. On the contrary, for wall suction (*Figure 12*), fluid is removed uniformly from the duct, and the skin friction coefficient decreases steadily downstream to zero where at that location the fluid is empty.

Note that, for all cases, a larger value of the flow index n gives rise to a larger skin friction coefficient. The reason for this phenomenon is that the apparent viscosity of a power-law non-Newtonian fluid is greater for a larger flow index n; therefore, the shear stress at the duct wall is larger for a larger n.

Pressure drop

In the present study, the dimensionless pressure drop is defined as $(p_o - p)/(1/2.\rho u_o^2)$, where p and p_o respectively denote the average pressure at each calculated point and at the inlet section. The distributions of pressure drop are shown in *Figures 13–15* for impermeable wall, wall blowing and wall suction, respectively.

In *Figure 13*, the pressure drops for an impermeable wall obtained by Doughty and Perkins[16] is given for comparison. The agreement between the present theory and the previous results is seen to be good. From the previous discussion, it has been indicated that the centreline velocity is greater for a larger flow index n; therefore, the average momentum at the same cross-section will be larger. By the conservation of momentum, a larger pressure drop is needed to maintain the fluid flow.

For wall blowing (*Figure 14*), as more and more fluid is injected into the duct, the net driving force in the flow direction must be increased continuously. That is, a larger pressure drop is needed to maintain an increased flow rate. The slope of the curve is increased along the flow direction. The agreement with previous results is found. That is because, for the blowing case, the length for flow to be fully-developed is much shorter, therefore, the entrance effect is small.

Figure 15 is presented for the case of wall suction. To test the validity of the prediction from boundary layer equations near the entrance for walls with blowing or suction, the result of Doughty and Perkins[16] is shown for comparison with the present results. The discrepancy is

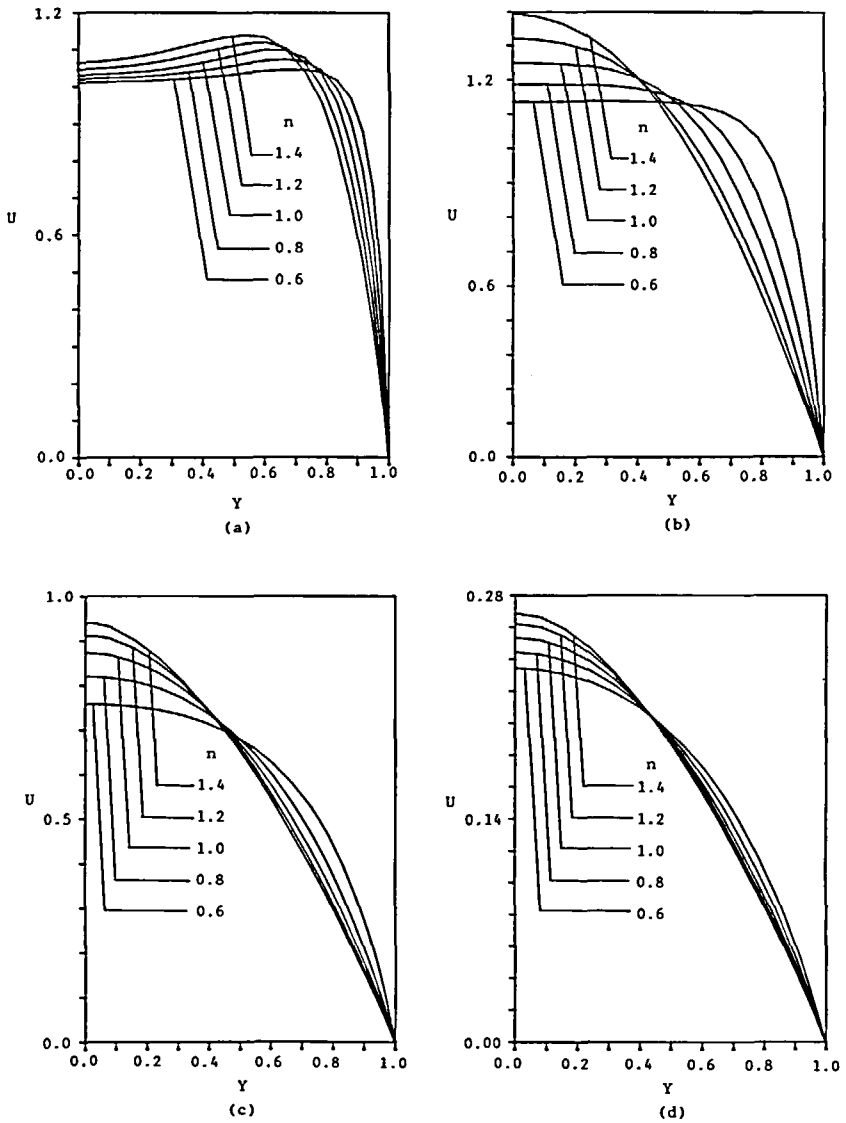

Figure 9 Velocity distributions for $V_w=0.04$ at (a) $X/Re=0.003457$; (b) the locations of maximum centreline velocity; (c) $X/Re=0.101386$; (*d*) $X/Re=0.207547$

found to be large. The Figure clearly shows the necessity of using the modified Navier–Stokes equations for these flow situations. From the momentum equations, it is known that the loss of momentum should be balanced by the gradients of pressure drop and wall skin friction. This also can be proved from *Figures 12* and *15*. From *Figure 12*, the wall skin friction is decreased gradually. Therefore, the pressure drop is increased to a maximum value and then decreased gradually, i.e., the pressure increased at the exit of duct. For small value of flow index n, the wall skin friction is small, then the pressure is raised more quickly, therefore, the negative pressure gradient can be found in the Figure.

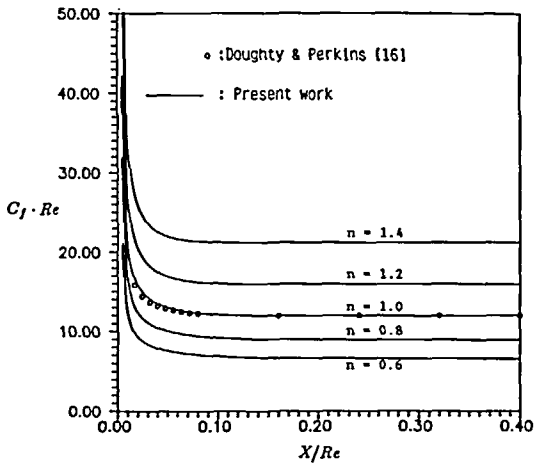

Figure 10 Distributions of skin friction coefficients; $V_w = 0$

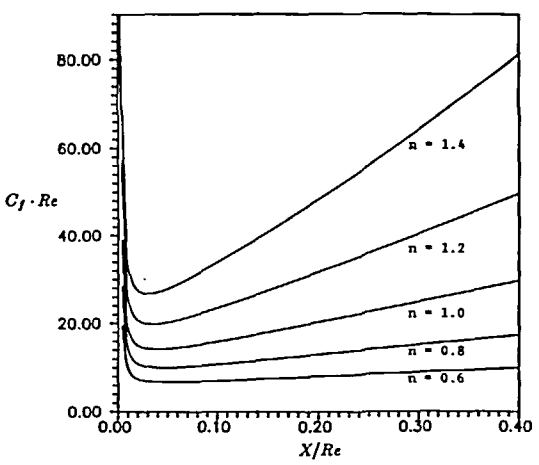

Figure 11 Distributions of skin friction coefficients; $V_w = -0.04$

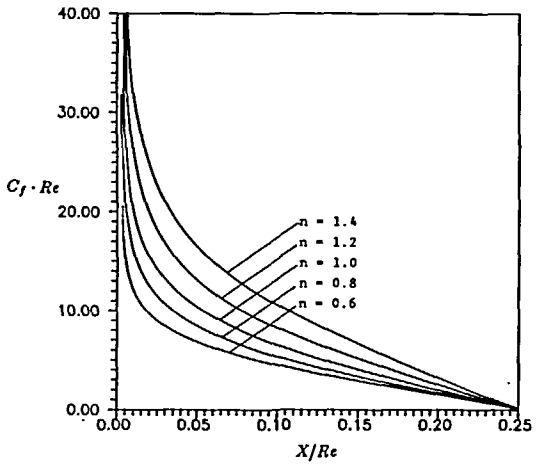

Figure 12 Distributions of skin friction coefficients; $V_w = 0.04$

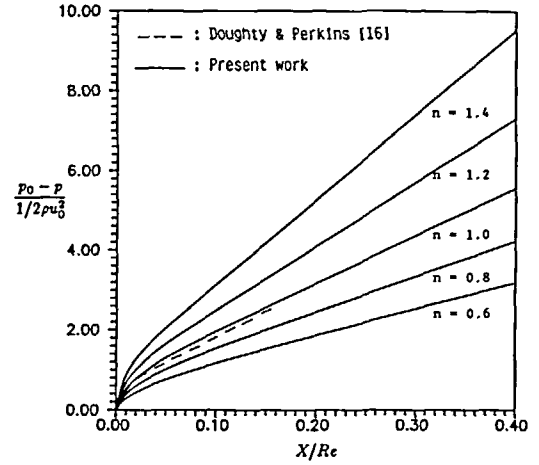

Figure 13 Distributions of pressure drop; $V_w = 0$

CONCLUSION

A numerical solution for the flow of a power-law fluid in the inlet region of a duct with blowing or suction has been obtained by solving the modified Navier–Stokes equations. Results for centre line velocity, axial velocity development, skin friction coefficients, and pressure drop are presented for a Reynolds number of 100. Cases of impermeable wall and wall with blowing or suction have been considered. Comparisons with available results lend support to the findings of the present investigation. The solution of boundary layer equations is shown not to be valid near the entrance, especially for blowing or suction. A velocity overshoot is found to be present in the near inlet region.

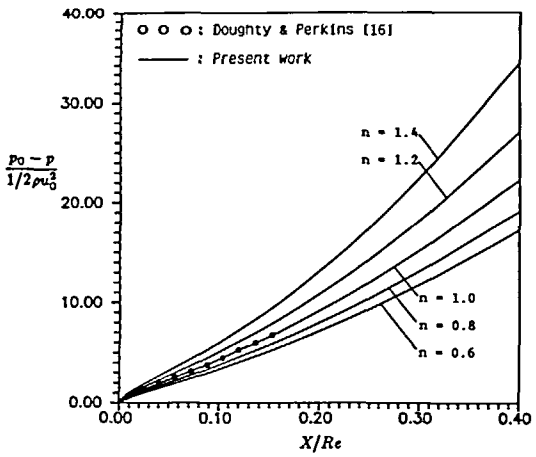

Figure 14 Distributions of pressure drop; $V_w = -0.04$

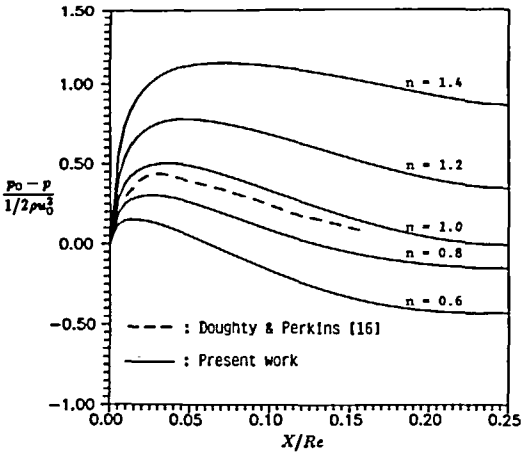

Figure 15 Distributions of pressure drop; $V_w = 0.04$

ACKNOWLEDGEMENTS

The authors wish to thank Professor C. K. Chen, Department of Mechanical Engineering, National Cheng-Kung University, Tainan, Taiwan, ROC and Dr. Win Aung, National Science Foundation, Washington, DC, USA, for helpful discussions and suggestions. The valuable comments given by reviewers are also very much appreciated.

REFERENCES

1 Langhaar, H. L. Steady flow in the transition length of a straight tube, *ASME J. Appl. Mech.*, **9**, 55–58 (1942)
2 Sparrow, E. M., Lin, S. H. and Lundgren, T. S. Flow development in the hydrodynamic entrance region of tubes and ducts, *Phys. Fluids*, **7**, 338–347 (1964)
3 Collins, M. and Schowalter, W. R. Behavior of non-Newtonian fluids in the inlet region of a channel, *AIChE J.*, **9**, 98–102 (1963)
4 Schiller, L. Die Entwicklung der laminaren Geschwindigkeits Verteilung ung ihre Bedeutung fur Zahigkeitmessungen, *Z. Angew. Math. Mech.*, **2**, 96–106 (1922)
5 Gupta, R. C. Entrance region flow of inelastic liquids, *J. Mecanique*, **8**, 207–214 (1969)
6 Tomita, Y. Analytical treatments of non-Newtonian fluid flow by introducing the conception of boundary layer, *Bull. JSME*, **4**, 77–86 (1961)
7 Duda, J. L. and Vrentas, J. S. Pressure losses in non-Newtonian flows, *Can. J. Chem. Eng.*, **50**, 671–674 (1972)
8 Hornbeck, R. W., Rouleau, W. T. and Osterle, F., Laminar entry problem in porous tubes, *Phys. fluids*, **6**, 1649–1654 (1963)
9 Wang, Y. L. and Longwell, P. A. Laminar flow in the inlet section of parallel plates, *AIChE. J.*, **10**, 323–329 (1964)
10 McDonald, J. W., Denny, V. E. and Mills, A. F. Numerical solutions of the Navier–Stokes equations in inlet regions, *ASME J. Appl. Mech.*, 39, 873–878 (1972)
11 Koyari, Y., Yoshizawa, A. and Takano, A. Studies on the starting flow and inlet flow in a channel and a pipe, *AIAA 14th Fluid Plasma Dynamics Conf., California*, Paper AIAA-81-1221 (1981)
12 Lenk, R. S. *Polymer Rheology*, Applied Science, London, (1978)
13 Raithby, G. D. and Knudsen, D. C. Hydrodynamic development in a duct with suction and blowing, *ASME J. Appl. Mech.*, **41**, 896–902 (1974)
14 Patankar, S. V. *Numerical Heat Transfer and Fluid Flow*, Hemisphere, New York (1980)
15 Skelland, A. H. P. *Non-Newtonian Flow and Heat Transfer*, John Wiley, New York (1967)
16 Doughty, J. R. and Perkins, H. C. Hydrodynamic entry length for laminar flow between parallel porous plates, *ASME J. Appl. Mech.*, **2**, 548–550 (1970)